

# Symmetrical acceptor-donor-acceptor type benzodithiophene based organic semiconductors for solution processed bulk heterojunction solar cells: optimization of open-circuit photovoltage with long alkyl group

WENQIN LI<sup>a,\*</sup>, ZIHUA WU<sup>a</sup>, MIN WU<sup>b</sup>, XIONGMIN CAI<sup>a</sup>, JINMIN WANG<sup>a,\*</sup>

<sup>a</sup>*School of Environmental and Materials Engineering, College of Engineering, Shanghai Polytechnic University, Shanghai 201209, China*

<sup>b</sup>*Department of Chemistry and Molecular Biology, University of Gothenburg, 40530, Göteborg, Sweden*

Symmetrical acceptor-donor-acceptor type benzodithiophene cored organic semiconductor with cyclopentadithiophene as  $\pi$  bridge, rhodanine as end group was synthesized. Their optical, electrochemical properties and photovoltaic performance acting as donor material in solution processed bulk heterojunction (BHJ) organic solar cells were investigated systematically. Theory calculation study was performed using density functional (DFT) and TD-DFT. WS-53 exhibited an ideal absorption profile in chloroform, with a theory voltage of 1.17 V for WS-53/PC<sub>71</sub>BM based BHJ solar cells. Under annealing treatment at 80°C, an overall power conversion efficiency of 1.04% was obtained with photocurrent density of 4.25 mA cm<sup>-2</sup> and voltage of 0.94 V.

(Received February 27, 2017; accepted November 28, 2017)

*Keywords:* BHJ solar cells, A-D-A type semiconductors, Benzodithiophene, Cyclopentadithiophene

## 1. Introduction

Organic bulk heterojunction (BHJ) solar cells have received world-wide attention due to their low cost, easy fabrication, lightweight properties and potential application in building-integrated photovoltaic system [1, 2]. Blended materials are always utilized as photo active layer in BHJ solar cells to deduce diffusion length, with polymer or small molecular semiconductors as donor and soluble fullerene as acceptor [3-5]. With respect to polymer based BHJ solar cells, solution processed small molecule semiconductors have emerged as competitive alternatives due to their facial synthesis and molecular modification, environmental friendly property and good solubility [6,7]. Generally, an ideal organic donor material should possess a broad and intense absorption profile, high carrier transporting ability, suitable energy level, as well as excellent film-forming characteristics and compatibility to fullerene acceptor [8-10]. Molecular engineering through combination of electron donor (D) and acceptor (A) with A-D-A or D-A-D configuration can achieved above characteristics [11-14]. For A-D-A type molecular, the HOMO level is mainly dominated by the donor segment, while the LUMO is mainly depends on the acceptor moiety [15-17].

Benzodithiophene has been widely utilized as photovoltaic materials in polymer based BHJ solar cells due to its excellent electron affinity as well as easy

functionalization property [18-20]. Incorporation of  $\pi$  bridge such as thiophene or cyclopentadithiophene is beneficial to increase planarity and improve the charge transfer properties of resultant materials [21]. Accordingly, a A- $\pi$ -D- $\pi$ -A type donor material with benzodithiophene as electron-donating core, cyclopentadithiophene as  $\pi$ -bridge, rhodanine as ending acceptor was designed for BHJ solar cells based on following consideration. (i) The solubility and film-formation ability can be further improved by introducing two 2-ethylhexyloxy chains on benzodithiophene [22]. (ii) Cyclopentadithiophene was incorporated as  $\pi$  bridge, taking advantage of its relatively high coefficient and good co-planar, thus promoting an extensive  $\pi$ -conjugated region [23]. (iii) electron-withdrawing rhodanine was introduced to enhance intramolecular transfer process. The photovoltaic performance was investigated using this benzodithiophene-based small molecule as donor materials along with PC<sub>71</sub>BM as acceptor to fabricate solution processed BHJ solar cells. After anneal-treatment at 80°C, an overall conversion efficiency of 1.04% was obtained with photocurrent density of 4.25 mA cm<sup>-2</sup> and voltage of 0.94 V.

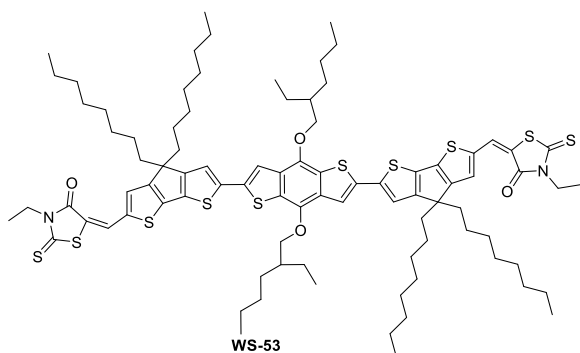


Fig. 1. Molecular structure of WS-53

## 2. Experimental section

### 2.1. Characterization

$^1\text{H}$  NMR and  $^{13}\text{C}$  NMR spectra were recorded on a Bruker AVANCE III HD 400 spectrometer using tetramethylsilane (TMS) as the internal standard. HRMS were recorded on a Waters LCT Premier XE instrument. The UV-Vis spectra were measured with a Varian Cary 100 spectrophotometer. The cyclic voltammogram was obtained with a Versastat II electrochemical workstation (Princeton Applied Research). Three-electrode cell was applied using a Pt disc working electrode with diameter of 3 mm, a Pt wire auxiliary electrode, and a saturated calomel electrode (SCE) reference electrode,  $0.1 \text{ mol}\cdot\text{L}^{-1}$  tetrabutylammonium-hexafluorophosphate ( $\text{TBAPF}_6$ ) in  $\text{CH}_3\text{Cl}$  was used as the supporting electrolyte. The scan rate was  $100 \text{ mV}\cdot\text{s}^{-1}$ . Photovoltaic measurements employed an AM 1.5 solar simulator equipped with a 300 W xenon lamp (model no. 91160, Oriel).  $I$ - $V$  curves were obtained by applying an external bias to the cell and measuring the generated photocurrent with a computer controlled Keithley 2400 source meter. The voltage step and delay time of the photocurrent were 10 mV and 40 ms, respectively.

### 2.2. General methods

All reagents and materials were commercial obtained unless otherwise specified. Tetrahydrofuran (THF) applied in Suzuki reaction was thoroughly dried with sodium. Dimethylformamide, dichloromethane and chloroform was pretreated with calcium hydride.

#### Synthesis of intermediate 2

Cyclopentadithiophene (1.0 g, 2.48 mmol), 1,2-dichloroethane (40 mL) and DMF (1 mL) were collected to 100 mL round-bottom flask under ice-bath to stirred for half an hour.  $\text{POCl}_3$  (700 mg) was added dropwise under argon atmosphere and kept for further 2h, then the mixture was warmed to room temperature and stirred overnight. Saturated sodium carbonate (25 mL) was added to the obtained mixture and stirred for 1h, followed

by extraction with dichloromethane. The organic phase was separated and removed through evaporation. A pale yellow power was obtained through column chromatography ( $\text{CH}_2\text{Cl}_2$ : petroleum ether = 1:3) in yield of 70.1%.  $^1\text{H}$  NMR (400 MHz,  $\text{CDCl}_3$ , ppm):  $\delta$  = 9.83 (s, 1H), 7.57 (s, 1H), 7.41 (d,  $J$  = 5.2 Hz, 1H), 6.99 (d,  $J$  = 4.8 Hz, 1H), 1.83-1.88 (m, 4H), 1.13-1.26 (m, 20H), 0.86-0.93 (m, 10H).  $^{13}\text{C}$  NMR (100 MHz,  $\text{CDCl}_3$ , ppm):  $\delta$  = 182.68, 162.47, 158.10, 147.76, 143.07, 135.53, 130.21, 129.61, 121.84, 53.73, 37.59, 31.77, 29.90, 29.29, 29.20, 24.55, 22.60, 14.09. HRMS (ESI,  $m/z$ ):  $[\text{M} + \text{H}]^+$  calcd for  $\text{C}_{26}\text{H}_{39}\text{OS}_2$ : 431.2442; found 431.2445.

#### Synthesis of intermediate 3

Compound 2 (900 mg, 2.09 mmol), THF (20 mL) were collected to a 100 mL round-bottom flask, NBS (1.87 g, 10.5 mmol) in THF (10 mL) was added slowly and stirred for 5h at room temperature. The reaction was quenched with water (50 mL) and extracted with dichloromethane ( $3\times 50$  mL). Organic phase was collected and evaporated under pressure. A pale yellow oil was obtained after column chromatography ( $\text{CH}_2\text{Cl}_2$ : petroleum ether = 1:2) in yield of 76.8%.  $^1\text{H}$  NMR (400 MHz,  $\text{CDCl}_3$ , ppm):  $\delta$  = 9.83 (s, 1H), 7.55 (s, 1H), 7.00 (s, 1H), 1.76-1.89 (m, 4H), 1.13-1.25 (m, 20H), 0.83-0.93 (m, 10H).  $^{13}\text{C}$  NMR (100 MHz,  $\text{CDCl}_3$ , ppm):  $\delta$  = 182.94, 161.38, 157.43, 147.09, 143.75, 136.19, 130.24, 125.21, 116.53, 54.87, 37.79, 32.06, 30.16, 29.57, 29.50, 24.81, 22.90, 14.38. HRMS (ESI,  $m/z$ ):  $[\text{M} + \text{H}]^+$  calcd for  $\text{C}_{26}\text{H}_{38}\text{BrOS}_2$ : 509.1547; found : 509.1551.

#### Synthesis of intermediate 5

Compound 3 (450 mg, 0.88 mmol), compound 4 (300 mg, 0.39 mmol), distilled toluene (50 mL) and  $\text{Pd}(\text{PPh}_3)_4$  (200 mg) were collected to 100 mL three-necked flask under argon atmosphere and reacted for 5h at  $100^\circ\text{C}$ . The mixture was poured to water (100 mL), extracted with dichloromethane ( $3\times 30$  mL). The organic phase was collected, dried with anhydrous sodium sulfate, and evaporated in *vacuo*. A red solid was afforded after column chromatography ( $\text{CH}_2\text{Cl}_2$ : petroleum ether = 1:1) in yield of 63.1%.  $^1\text{H}$  NMR (400 MHz,  $\text{CDCl}_3$ , ppm):  $\delta$  = 9.85 (s, 2H), 7.58 (s, 2H), 7.55 (s, 2H), 7.18 (s, 2H), 4.20 (d,  $J$  = 5.4 Hz, 4H), 1.84-1.98 (m, 10H), 1.70-1.77 (m, 2H), 1.61-1.69 (m, 4H), 1.43-1.47 (m, 9H), 1.14-1.27 (m, 42H), 1.05-1.10 (m, 7H), 0.96-1.01 (m, 12H), 0.81-0.86 (t,  $J$  = 6.8 Hz, 12H).  $^{13}\text{C}$  NMR (100 MHz,  $\text{CDCl}_3$ , ppm):  $\delta$  = 182.57, 163.05, 158.20, 147.12, 144.18, 143.79, 141.85, 136.84, 135.70, 132.56, 129.90, 129.18, 119.61, 116.23, 54.31, 40.70, 37.66, 31.78, 30.45, 29.93, 29.30, 29.23, 24.61, 23.87, 23.20, 22.60, 14.07, 11.38.

#### Synthesis of compound WS-53

Compound 5 (200 mg, 0.15 mmol), 3-ethylrhodanine (300 mg, 1.86 mmol), dried chloroform (50 mL) and piperidine (0.5 mL) were collected in a bottom flask under argon atmosphere to reflux for 48h. The obtained mixture

was poured into dichloroformmethane (50 mL), washed with brine. Organic phase was separated, dried with anhydrous sodium sulfate and evaporated *in vacuo*. A black solid was obtained after column chromatography ( $\text{CH}_2\text{Cl}_2$ : petroleum ether = 1:1) in yield of 54.6%. Further recrystallization was carried out to get black powder 100 mg.  $^1\text{H}$  NMR (400 MHz,  $\text{CDCl}_3$ , ppm):  $\delta$  = 7.85 (s, 2H), 7.43 (s, 2H), 7.24 (s, 2H), 7.16 (s, 2H), 4.20 (m, 8H), 1.86-1.99 (m, 8H), 1.84-1.88 (m, 4H), 1.72-1.80 (m, 6H), 1.65-1.69 (m, 4H), 1.44-1.50 (m, 8H), 1.15-1.24 (m, 42H), 1.07-1.12 (m, 8H), 0.99-1.03 (m, 12H), 0.81-0.85 (m, 12H).  $^{13}\text{C}$  NMR (100 MHz,  $\text{CDCl}_3$ , ppm):  $\delta$  = 191.62, 167.26, 161.89, 159.54, 145.96, 143.99, 141.45, 139.02, 136.80, 136.01, 132.52, 128.98, 127.99, 126.30, 119.48, 117.73, 115.93, 76.02, 54.36, 40.72, 39.97, 37.79, 31.79, 30.49, 29.97, 29.37, 29.27, 24.70, 23.90, 23.23, 22.63, 14.30, 14.09, 12.31, 11.43.

### 2.3. Device fabrication and characterization

BHJ solar cells were fabricated using a blended layer of WS-53 and  $\text{PC}_{71}\text{BM}$  as photo active layer, PEDOT:PSS (AI4083) as hole-transporting layer and LiF/Al as photocathode material. ITO conducting glass were thoroughly cleaned with glass cleaner, deionized water, acetone and isopropyl alcohol respectively through ultrasonic washer. PEDOT: PSS (Clevios P VP AI4083, 0.45  $\mu\text{m}$ ) was spin-coated to ITO glass at speed of 3000 rpm. After dried at 150°C for 20 min, the electrode was transferred to glove box under atmosphere of argon. A mixture of WS-53 and  $\text{PC}_{71}\text{BM}$  (1:0.8, weight ratio; concentration of WS-53, 8 mg/mL) in chloroform was spin coated on top of hole-transporting layer, with thickness of 100 $\pm$ 10 nm. The obtained electrode was further modified with 0.8 nm LiF and 80 nm Al through vacuum evaporation, the operating vacuum pressure was below 200  $\mu\text{Pa}$ , with effective area of 4  $\text{mm}^2$ .

### 2.4. Computation methods

All the calculations are performed in Gaussian09 software package. The gas-phase ground state geometry optimizations were performed using the B3LYP functional, which consists of Beck's three parameter gradient-corrected exchange functional and Lee-Yang-Parr correlation functional, along with the 6-31+G(d,p) basis set. Frequency calculations at the same level of theory have also been performed to identify all the stationary points as minima (zero imaginary frequency) and to provide free energies at 298.15 K, which include entropic contributions by taking into account the vibrational, rotational, and translational motions of the species under consideration [24]. The time-dependent density functional theory (TD-DFT) was adopted at the same level to estimate the excitation energies.

## 3. Results and discussion

### 3.1. Synthesis

The synthesis routes were outlined in Fig. 2. Vilsmeier reaction of cyclopentadithiophene was carried out to obtain the aldehyde form imdiate 2. Compound 3 was synthesized through radical substitution reaction with *N*-bromosuccinimide. To be mentioned, the reaction and post-processing of abovementioned two reactions should be carried out under room temperture due to instability of cyclopentadithiophene under heat. Compound 5 was synthesized through stille coupling reaction between compound 3 and 2,2'- cyclopentadithiophene selenide reagents. Organic semiconductor **WS-53** was obtained through traditional Knoevenagel condensation reaction. The structure of important imdicates were identified with  $^1\text{H}$  NMR,  $^{13}\text{C}$  NMR and HR-MS.

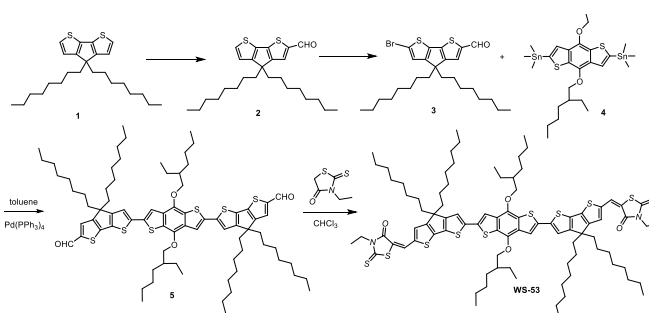


Fig. 2. Synthetic procedure of **WS-53**

### 3.2. Optical property

Fig. 3 depicts the absorption spectra of **WS-53** in chloroform and on film blended with  $\text{PC}_{71}\text{BM}$ . The optical parameters were shown in Table 1. **WS-53** exhibits a broad and intense absorption profile in chloroform, with a relatively low energy band gap of 1.84 eV and coefficient of  $13.2 \times 10^4 \text{ M}^{-1} \cdot \text{cm}^{-1}$ . Obviously, the incorporation of cyclopentadithiophene on the side of benzodithiophene is beneficial to electron delocalization as well as light-harvesting ability of resultant **WS-53**. When coated on film blended with  $\text{PC}_{71}\text{BM}$ , a red-shifted absorption threshold and broaden absorption profile can be observed due to  $\pi$ - $\pi$  aggregation during film-formation process. The absorption spectra were well overlapped with entire visible region, indicative of excellent light harvesting ability of **WS-53** based BHJ solar cells.

### 3.3. Electrochemical property

As ideal donor materials, suitable energy levels are also key parameters influencing the photovoltaic performance. The LUMO level should be well matched with LUMO of the acceptor materials to guarantee efficient exciton dissociation. While theory voltage of BHJ solar cells is determined by the differences between the HOMO level of

donor materials and LUMO of PC<sub>71</sub>BM. Accordingly, electrochemical measurement was carried out to quantify the energy level assuming the energy level of ferrocene/ferrocenium (Fc/Fc<sup>+</sup>) to be -4.8 eV. The HOMO value corresponded to first redox potential, which was recalculated with onset of the first oxidation. While the LUMO was calculated according to equation of LUMO=HOMO- $E_{0,0}$ . Accordingly, the HOMO and LUMO of **WS-53** were determined to be -5.17 eV and -3.33 eV, respectively, with energy gap of 1.84 eV. The electron driving force between LUMO level of donor material and PC<sub>71</sub>BM (-4.0 eV) is greater than exciton binding energy of 0.3 eV, ensuring efficient exciton dissociation to LUMO of PC<sub>71</sub>BM. The theory voltage for **WS-53**/PC<sub>71</sub>BM based BHJ solar cells is 1.17 V.

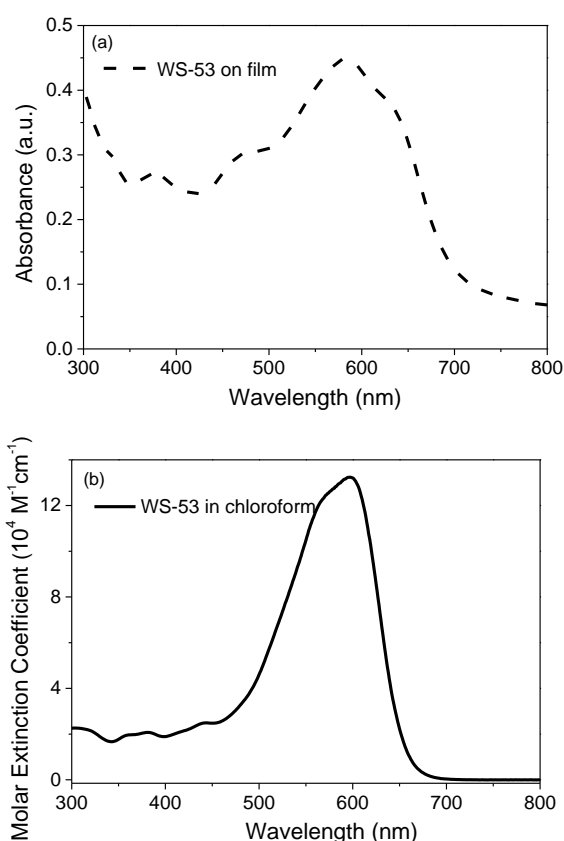


Fig. 3. UV-vis absorption spectra of **WS-53**. (a) in chloroform, (b) on film blended with PC<sub>71</sub>BM

### 3.4. Density functional theory calculations

Moreover, theoretical study was performed using DFT and TD-DFT. The frontier orbitals with iso-value = 0.02 are plotted in Fig. 5. The HOMO orbital was delocalized throughout the whole molecules. Whereas for the HOMO-1, LUMOs and LUMO+1 are mainly distribute on the two acceptor ends of structure, a small parts distribute on donor core. The first excitation is mainly originated by electron transition from HOMO to LUMO level, while the smaller absorption shoulder located in shorter wavelength is mainly

caused by electron transition between HOMO-1 and LUMO+1 level.

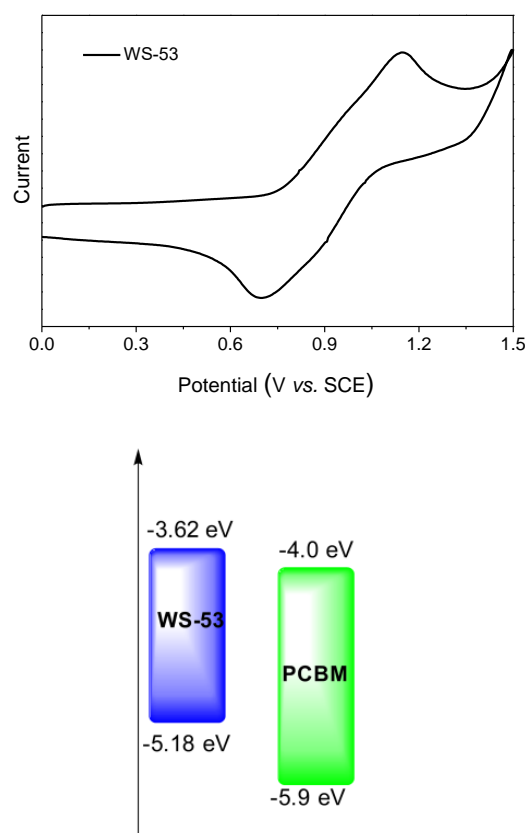


Fig. 4. Cyclic voltammetry plots of **WS-53** in CHCl<sub>3</sub> and HOMO-LUMO alignment to PC<sub>71</sub>BM

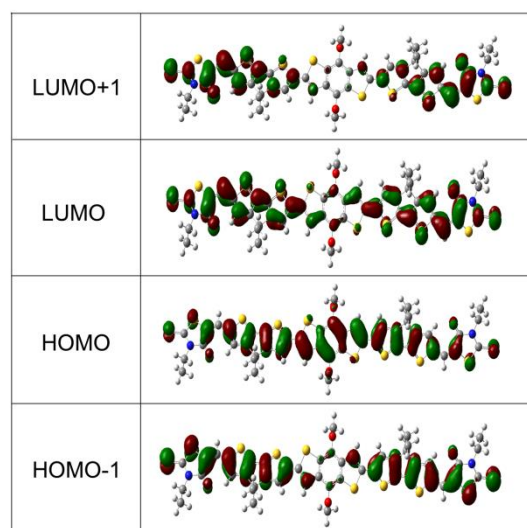


Fig. 5. HOMO-1, HOMO, LUMO and LUMO+1 orbitals of **WS-53**. Note: The methoxyl group was used instead of the 2-ethyl-hexoxyl group to simplify calculation

Table 1. Photophysical and electrochemical parameters of WS-53

Compound	$\lambda_{\max}$ (nm)		$\epsilon_{\text{solution}}$ ( $\text{M}^{-1}\cdot\text{cm}^{-1}$ )	$E_{\text{g}}^{\text{opt b}}$ (eV)	$E_{\text{ox}}$ (V)	HOMO (eV)	LUMO (eV)
	Solution <sup>a</sup>	Film					
<b>WS-53</b>	597	582	$13.2 \times 10^4$	1.84	0.93	-5.17	-3.33

<sup>a</sup>Absorption data was measured in  $\text{CHCl}_3$  solution and on film blended with  $\text{PC}_{71}\text{BM}$ .

<sup>b</sup> $E_{\text{g}}^{\text{opt}}$  was calculated with absorption threshold on film according equation  $E_{\text{g}}^{\text{opt}} = 1240/\lambda$ .

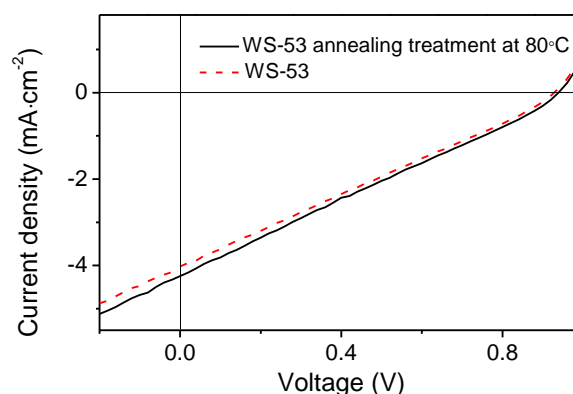
<sup>c</sup> $E_{\text{ox}}$  and HOMO level were obtained through electrochemical measurement with three-electrode system in  $\text{CHCl}_3$  solution, ferrocene was used as external standard.

Table 2. Optical properties of WS-53 calculated at TD-B3lyp/6-31+G(d,p) level. Specifically the wavelengths of absorbance peak  $\lambda_{\max}$  with corresponding oscillator (O.S.) and main contributions

Molecule	Absorption (nm)	Oscillator strength	Orbitals
<b>WS-53</b>	676.30	3.6319	HOMO-1 $\rightarrow$ LUMO+1 (12.5%)
			HOMO $\rightarrow$ LUMO (87.5 %)
	509.01	0.9328	HOMO-1 $\rightarrow$ LUMO+1 (74.4%)
			HOMO $\rightarrow$ LUMO (12.8 %) HOMO $\rightarrow$ LUMO+2 (12.8 %)

### 3.5. Photovoltaic property

BHJ solar cells were fabricated using blended layer of **WS-53** and  $\text{PC}_{71}\text{BM}$  as photo active layer, with weight ratio of 1:0.8. The obtained current density-voltage ( $J$ - $V$ ) curve and corresponding photovoltage parameters are listed in Table 3. The BHJ solar cells show a relatively high voltage of  $\sim 0.93$  V due to its deeper HOMO level, which is originated by excellent electron donating ability of benzodithiophene. Annealing treatment at  $80^\circ\text{C}$  was carried out to enhance charge transfer ability [25]. As shown in Fig. 6, an improvement in photovoltaic performance was realized with photocurrent density of  $4.25 \text{ mA cm}^{-2}$  and voltage of  $0.94$  V.

Fig. 6.  $J$ - $V$  curves of solar cells with an active layer composed of **WS-53**/ $\text{PC}_{71}\text{BM}$ (1:0.8w/w)Table 3. Photovoltaic performance of BHJ solar cells based on **WS-53**

Active layer	Ratio	$V_{\text{oc}}$ (V)	$J_{\text{sc}}$ ( $\text{mA}\cdot\text{cm}^{-2}$ )	$FF$ (%)	PCE (%)
<b>WS-53</b> / $\text{PC}_{71}\text{BM}$	-	0.93	3.98	26.0	0.96
<b>WS-53</b> / $\text{PC}_{71}\text{BM}$ annealed at $80^\circ\text{C}$	1: 0.8	0.94	4.25	25.7	1.04

### 4. Conclusion

The synthesis of symmetrical A-D-A type electron donor material **WS-53** using benzodithiophene as electron-donating core, cyclopentadithiophene as  $\pi$ -bridge, rhodanine as ending acceptor was reported. 2-ethyl-hexoxyl and octyl were incorporated to improve the solubility and

film-forming ability. The optical ability both in solution and on film blended with  $\text{PC}_{71}\text{BM}$  as well as electrochemical property were carried out to quantify the energy level. Photovoltaic performance measurement in BHJ solar cells using **WS-53** as donor material, along with  $\text{PC}_{71}\text{BM}$  as acceptor were performed. Our result indicated that incorporation of benzodithiophene can significant broaden

optical response as well as enhance absorption ability. A relatively higher voltage was obtained due to its deeper HOMO level and larger theory open-circuit voltage. An overall conversion efficiency of 1.04% was obtained under optimization, with photocurrent density of  $4.25 \text{ mA cm}^{-2}$ , open circuit voltage of 0.94 V and fill factor of 25.7%.

### Acknowledgments

This work was financially supported by the NSFC/China (No. 61376009, 51590902), and Oriental Scholarship, Science and Technology Commission of Shanghai Municipality (14YF1410500), "Shu Guang" project (No. 13SG55), and Key Subject of Shanghai Polytechnic University (Material Science and Technology, XXXKZD1601).

### References

- [1] J. W. Jo, M.-S. Seo, M. Park, J.-Y. Kim, J. S. Park, I. K. Han, H. Ahn, J. W. Jung, B.-H. Sohn, M. J. Ko, H. J. Son, *Adv. Funct. Mater.* **26**(25), 4464 (2016).
- [2] M. A. Alam, B. Ray, M. R. Khan, S. Dongaonkar, *J. Mater. Res.* **28**(4), 541 (2013).
- [3] J. Min, Y. N. Luponosov, N. Gasparini, M. Richter, A. V. Bakirov, M. A. Shcherbina, S. N. Chvalun, L. Grodd, S. Grigorian, T. Ameri, S. A. Ponomarenko, C. J. Brabec, *Adv. Energy Mater.* **5**(17), 1500386 (2015).
- [4] M. Li, F. Liu, X. Wan, W. Ni, B. Kan, H. Feng, Q. Zhang, X. Yang, Y. Wang, Y. Zhang, Y. Shen, T. P. Russell, Y. Chen, *Adv. Mater.* **27**(40), 6296 (2015).
- [5] Y. Zhang, J. Liu, N. Thuc-Quyen, *ACS Appl. Mat. Interfaces* **5**(7), 2347 (2013).
- [6] M. Cheng, C. Chen, X. C. Yang, J. Huang, F. G. Zhang, B. Xu, L. C. Sun, *Chem. Mat.* **27**(5), 1808 (2015).
- [7] S. Paek, J. K. Lee, J. Ko, *Sol. Energy Mater. Sol. Cells* **120**(Part A), 209 (2014).
- [8] M. L. Keshtov, D. Y. Godovsky, S. A. Kuklin, J. Lee, J. Kim, B. Lim, H. K. Lee, S. Biswas, E. N. Koukaras, G. D. Sharma, *Dyes Pigments* **132**, 387 (2016).
- [9] N. Kim, S. Park, M.-H. Lee, J. Lee, C. Lee, S. C. Yoon, *J. Nanosci. Nanotechnol.* **16**(3), 2916 (2016).
- [10] J. Kwon, T.-M. Kim, H.-S. Oh, J.-J. Kim, J.-I. Hong, *Rsc. Advances* **4**(47), 24453 (2014).
- [11] J. Min, Y. N. Luponosov, N. Gasparini, L. W. Xue, F. V. Drozdov, S. M. Peregodova, P. V. Dmitryakov, K. L. Gerasimov, D. V. Anokhin, Z. G. Zhang, T. Ameri, S. N. Chvalun, D. A. Ivanov, Y. F. Li, S. A. Ponomarenko, C. J. Brabec, *J. Mater. Chem. A* **3**(45), 22695 (2015).
- [12] K. Wang, R.-Z. Liang, J. Wolf, Q. Saleem, M. Babics, P. Wucher, M. Abdelsamie, A. Amassian, M. R. Hansen, P. M. Beaujuge, *Adv. Funct. Mater.* **26**(39), 7103 (2016).
- [13] N. F. Montcada, S. Arrechea, A. Molina-Ontoria, A. I. Aljarilla, P. de la Cruz, L. Echegoyen, E. Palomares, F. Langa, *Org. Electron.* **38**, 330 (2016).
- [14] C. Zhong, J. A. Bartelt, M. D. McGehee, D. Can, F. Huang, Y. Cao, A. J. Heeger, *J. Phys. Chem. C* **119**(48), 26889 (2015).
- [15] J. E. Coughlin, Z. B. Henson, G. C. Welch, G. C. Bazan, *Accounts Chem. Res.* **47**(1), 257 (2014).
- [16] Y. Patil, R. Misra, A. Sharma, G. D. Sharma, *Phys. Chem. Chem. Phys.* **18**(25), 16950 (2016).
- [17] L. Xiao, H. Wang, K. Gao, L. Li, C. Liu, X. Peng, W.-Y. Wong, W.-K. Wong, X. Zhu, *Chem-Asian J.* **10**(7), 1513 (2015).
- [18] J. Du, A. Fortney, K. E. Washington, C. Bulumulla, P. Huang, D. Dissanayake, M. C. Biewer, T. Kowalewski, M. C. Stefan, *ACS Appl. Mat. Interfaces* **8**(48), 33025 (2016).
- [19] S. Goker, G. Hizalan, E. Aktas, S. Kutkan, A. Cirpan, L. Toppare, *New J. Chem.* **40**(12), 10455 (2016).
- [20] T. Kastinen, M. Niskanen, C. Risko, O. Cramariuc, T. I. Hukka, *J. Phys. Chem. A* **120**(7), 1051 (2016).
- [21] W. W. Zhang, Y. Z. Wu, H. B. Zhu, Q. P. Chai, J. C. Liu, H. Li, X. R. Song, W. H. Zhu, *ACS Appl. Mat. Interfaces* **7**, 26802 (2015).
- [22] B. Qiu, J. Yuan, Y. Zou, D. He, H. Peng, Y. Li, Z. Zhang, *Org. Electron.* **35**, 87 (2016).
- [23] Q. P. Chai, W. Q. Li, J. C. Liu, Z. Y. Geng, H. Tian, W. H. Zhu, *Sci. Rep.* **5**, 11 (2015).
- [24] J. Vega-Guzman, A. A. Alshaery, E. M. Hilal, A. H. Bhrawy, M. F. Mahmood, L. Moraru, A. Biswas, A. Popa, *J. Optoelectron. Adv. M.* **16**, 1063 (2014).
- [25] C. D. Wessendorf, G. L. Schulz, A. Mishra, P. Kar, I. Ata, M. Weidener, M. Urdanpilleta, J. Hanisch, E. Mena-Osteritz, M. Lindén, E. Ahlswede, P. Bäuerle, *Adv. Energy Mater.* **4**(14), 1300626 (2014).

\*Corresponding author: wqli@sspu.edu.cn,  
wangjinmin@sspu.edu.cn